Received: 25 August 2021 | Revised: 30 October 2021 | Accepted: 28 November 2021

DOI: 10.1002/jcc.26797

RESEARCH ARTICLE

Journal of COMPUTATIONAL CHEMISTRY WILEY

Using projection operators with maximum overlap methods to simplify challenging self-consistent field optimization

Hector H. Corzo | Ali Abou Taka | Aurora Pribram-Jones | Hrant P. Hratchian

Department of Chemistry and Biochemistry and Center for Chemical Computation and Theory, University of California, Merced, California, USA

Correspondence
Aurora Pribram-Jones and Hrant P. Hratchian, Department of Chemistry and Biochemistry and Center for Chemical Computation and Theory, University of California, Merced, CA 95343, USA.
Email: apj@ucmerced.edu and hhratchian@ucmerced.edu

Funding information
Division of Chemistry, Grant/Award Number: 1848580; U.S. Department of Energy, Grant/Award Number: DE-SC0014437

[Correction added on 24 Feb 2022, after the first online publication: typographical errors in equations 2 and 3, and in 7th line in introduction section, and formatting error in table 1 have been corrected.]

Abstract

Maximum overlap methods are effective tools for optimizing challenging ground- and excited-state wave functions using self-consistent field models such as Hartree-Fock and Kohn-Sham density functional theory. Nevertheless, such models have shown significant sensitivity to the user-defined initial guess of the target wave function. In this work, a projection operator framework is defined and used to provide a metric for non-aufbau orbital selection in maximum-overlap-methods. The resulting algorithms, termed the Projection-based Maximum Overlap Method (PMOM) and Projection-based Initial Maximum Overlap Method (PIMOM), are shown to perform exceptionally well when using simple user-defined target solutions based on occupied/virtual molecular orbital permutations. This work also presents a new metric that provides a simple and conceptually convenient measure of agreement between the desired target and the current or final SCF results during a calculation employing a maximum-overlap method.

KEYWORDS
excited state, maximum overlap method, self-consistent field

1 | INTRODUCTION

Efficient and reliable methods for studying excited electronic states and exotic ground state problems are essential for the application of electronic structure theory to frontier problems in chemistry. In the last few decades, computational chemistry has experienced extraordinary advances in ground state and excited state methodologies.[1–7] In particular, ground state Kohn-Sham (KS) Density Functional Theory (DFT) and linear response time dependent Density Functional Theory (TD-DFT) have become the workhorses of modern computational chemistry. Despite these advancements, practitioners often experience significant challenges with both ground and excited state calculations. In many cases, the desired electronic structure can be quite challenging to locate as part of standard self–consistent field (SCF) optimizations, if not entirely elusive. Without a reliable methodology or metric to guide these choices, such studies often rely on equal parts science and art by the practitioner.

With respect to electronic excited states, single reference models are often preferred due to their attractive computational scaling and conceptual advantages. For example, methods such as configuration–interaction with singles substitutions (CIS) and (linear response) TD-DFT are among the most commonly used models for characterizing excited states of molecules.[8–24] In particular, the approximate inclusion of electron correlation effects and its computational feasibility have made TD-DFT the most widely used method for calculating excited states energies.

Despite its success, popularity, and broad applicability, TD-DFT has a number of challenges. Current TD-DFT approximations give significant errors for excited states arising from π–electron excitations[25,26] and may not accurately describe charge–transfer (CT) processes.[27–29] For such cases, where many TD-DFT approximations fail to correctly describe molecular systems, excited state approximations based on SCF solutions offer an attractive alternative for characterizing these cases. Different excited states may be approximated by independent SCF solutions. Thus, the excitation energy between two electronic states can be given by the energy

Hector H. Corzo and Ali Abou Taka contributed equally to this work.

difference between two distinct SCF solutions. This approach for computing excited state energies is often referred to as the Δ-SCF approximation. KS-DFT Δ-SCF methods, unlike traditional TD-DFT methods, have the advantage of accounting for orbital relaxation corrections, which can be as important as the electron–electron correlation correction.

Following a Δ-SCF strategy for the description of excited states, a number of different approaches for reliably finding SCF solutions describing excited states have appeared in the literature.[30–39] Recently, the maximum overlap method (MOM) has received increasing interest.[40–42] MOM and the related initial maximum overlap method (IMOM) have shown great success in converging solutions that correspond to specific electronic excited states. In these methodologies, molecular orbital occupation in the SCF procedure is dictated by a measure of overlap between the occupied orbitals of successive SCF iterations (or with the initial guess), instead of the standard orbital eigenvalue-based aufbau principle.

MOM-based approaches have been applied to core-level excitation energies, valence excitations, and excited state geometries.[40–42] Despite these successes, such methods can be quite sensitive to the initial guess and the employed SCF optimization algorithm. Thus, the likelihood of optimizing to the desired non-aufbau solution can be highly user-dependent. Responding to this observation, multiple groups have proposed alternative algorithms for driving SCF searches to non-aufbau solutions. Two recent algorithms are the squared–gradient minimization (SGM)[43] and the state–targeted energy projection (STEP).[44] In the SGM approach, the saddle-point optimization is reframed as a minimization problem by optimizing the square of the orbital gradient rather than the energy Lagrangian. This approach may avoid variational collapse in the SCF procedure; however, the method is a factor of 2–3 more computationally expensive than the traditional SCF algorithm and may converge to solutions that do not correspond to stationary points in SCF space. The second recent alternative, STEP, is closely related to the Big Shift method previously developed by Zerner and co-workers.[39] STEP and Big Shift schemes decrease occupied–virtual rotations during SCF iterations by introducing a modified level shift to guide the molecular orbital (MO) optimization toward a target solution.

A primary attraction of MOMs is the simplicity of the approach. Indeed, most MOMs can be integrated into existing SCF programs with only minor changes and then used directly with SCF gradient, hessian, and property codes. Nevertheless, there are important and recognized limitations with MOMs. Whereas the recent literature thoroughly demonstrates the successful use of such models,[40–43,45] a remaining challenge is the documented dependence of SCF success on the definition of the modified aufbau metric and the initial guess (vide infra).[35,38,39,43,46–50]

In this work, we examine the use of MOM and IMOM approaches with a modified aufbau metric based on a projection operator describing a target density in the basis of the current MOs at each SCF iteration. We refer to resulting variants as projection maximum overlap method (PMOM) and projection initial maximum overlap method (PIMOM). As shown below, the construction of a modified aufbau metric for SCF calculations based on a projection framework rather than an overlap picture yields an effective, robust, and conceptually pleasing alternative to other metrics. As discussed below, we measure SCF optimization success from a user-provided guess wave function formulated as simple MO permutations on an initial ground state calculation. Based on the PMOM/PIMOM formulation, we also provide a convenient diagnostic metric, N_{virt}, describing the agreement between target and final converged states.

2 | METHODS

As mentioned above, using MOM-like approaches to drive SCF solvers toward a solution resembling a target electronic structure has been demonstrated in the literature for some time.[33,35,39–42,47,51–58] In this section, we describe our construction of a projection-based framework and a proposed metric for quantitatively assessing the relationship between target and current electronic structures (either specific iterations during the SCF procedure or the converged SCF result). For the remainder of this section, indices employ a standard convention.[59] Specifically, Greek letters are used to denote atomic orbital (AOs) and Roman letters denote MOs. MO. indices $i,j,k,\ldots$ denote occupied MOs; $a,b,c,\ldots$ denote virtual MOs; and $p,q,r,\ldots$ denote all (both occupied and virtual) MOs. In what follows, the MO coefficients for the target and current electronic structures are given by matrices $\mathbf{C}^{\text{target}}$ and $\mathbf{C}$; the AO overlap matrix is given by matrix $\mathbf{S}$.

This work focuses on two recent categories of maximum overlap methods.[40–42] The first category uses the occupied molecular orbitals generated in each SCF cycle as the target state for the next SCF cycle—referred to as MOM. The second approach uses the initial guess, often prepared by a user from a previous calculation, as a pinned target for all SCF cycles—referred to as IMOM. In both cases, the SCF procedure is carried out using a modified aufbau principle where a measure of overlap, or agreement, of each MO with the target state, is used in lieu of the canonical MO Fock eigenvalues.

The modified aufbau rule used in MOM schemes can be defined according to an ordered list of metrics, $\{s_p\}$. In general, this list aims to quantify the overlap of each current MO with the occupied MO sub-space of the target state. Figure 1 shows a flowchart demonstrating a standard MOM algorithm. As shown, the algorithm starts with an initial guess that is typically provided by the user and often models a desired electronic excited state. This initial guess provides the atomic overlap and the molecular coefficients that are used to define the projector that is used in each SCF iteration. After the projection of the current SCF state the orbitals are re-arranged and the convergence of the SCF is tested; the process repeats until convergence is met.

A variety of $\{s_p\}$ definitions have appeared in the literature. Three such definitions include giving $\{s_p\}$ as the sum of target–occupied–MO/current–Mo overlap elements,[42,57]

$$s_p = \sum_i {}^{i^{\text{target}}} \langle p \rangle = \sum_{\mu\nu} \sum_{i^{\text{target}}} C_{\mu i}^{\text{target}} S_{\mu\nu} C_{\nu p}, \tag{1}$$

as the square root of the previous sum,[41]

$$s_p = \left(\sum_i \langle i^{\text{target}} | p \rangle \right)^{1/2} = \left(\sum_{\mu\nu} \sum_{i^{\text{target}}} C_{\mu i}^{\text{target}} S_{\mu\nu} C_{\nu p} \right)^{1/2}, \quad (2)$$

and as the square-root of the sum of squared target occupied MO/current MO overlap integrals.[40]

$$s_p = \left(\sum_i |\langle i^{\text{target}} | p \rangle|^2 \right)^{1/2} = \left[\sum_{\mu\nu} \sum_{i^{\text{target}}} \left(C_{\mu i}^{\text{target}} S_{\mu\nu} C_{\nu p} \right)^2 \right]^{1/2}. \quad (3)$$

The non-aufbau metric given by Equation (1) is based on identifying MOs at each SCF cycle that exhibit the greatest *overlap* with the occupied MOs comprising the target determinant. One issue that arises with that straightforward expression is signed overlap values due to the arbitrary phase of Fock matrix eigenvectors. In principle, all metrics based on such an overlap framework will be affected by the phase issue. Indeed, Equation (3) essentially evaluated the sum of absolute overlaps, which is a simple means for removing phase complications.

As an alternative construction for the modified aufbau metric, s_p, we began by asking which set of current Fock eigenvectors can be used to construct a determinant with the largest projection onto the target determinant. We refer to this approach as PMOM (or PIMOM when the target is the initial determinant). The PMOM/PIMOM scheme begins by defining the target system's density operator, $\mathcal{P}^{\text{target}}$, which projects a ket onto the occupied MO space of the target system,

$$\mathcal{P}^{\text{target}} = \sum_i |\, i^{\text{target}} \rangle \langle i^{\text{target}} \,|. \quad (4)$$

This projection operator can be represented in the basis of the current MOs at each SCF cycle as

$$P_{pq}^{\text{target}} = \langle p | \mathcal{P}^{\text{target}} | q \rangle = \sum_i \langle p | i^{\text{target}} \rangle \langle i^{\text{target}} | q \rangle. \quad (5)$$

Note that both occupied and virtual current-cycle SCF MOs are necessary to provide a complete basis. When the SCF procedure is carried out in the AO basis, Equation (5) is given by

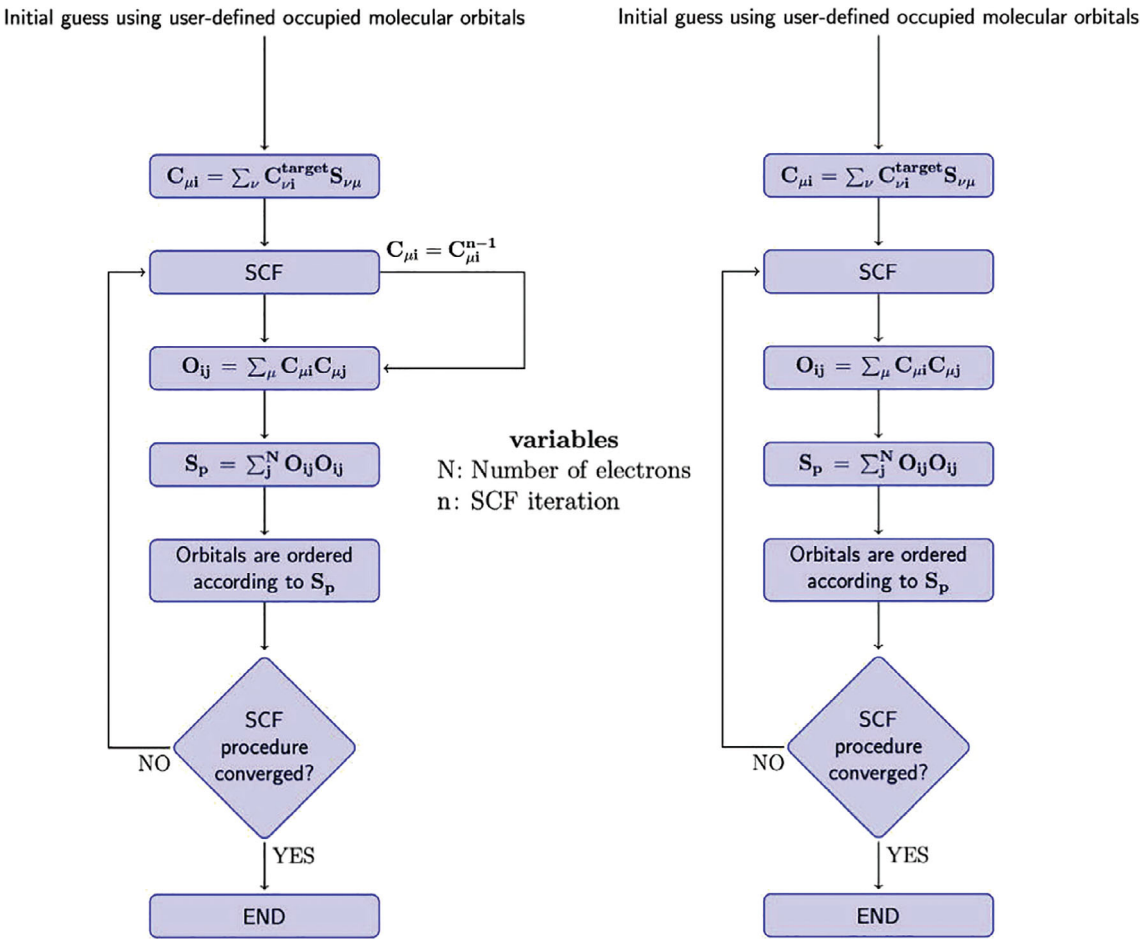

FIGURE 1 Standard PMOM (left)/PIMOM (right) SCF algorithm flowcharts

$$P_{pq}^{target} = \sum_{i} \sum_{\mu\nu} \sum_{\lambda\sigma} C_{\mu p} S_{\mu\lambda} C_{\lambda i}^{target} C_{\sigma i}^{target} S_{\sigma\nu} C_{\nu q}, \quad (6)$$

where C, C^{target}, and S are the current set of MO coefficients, target system MO coefficients, and the AO overlap matrix, respectively.

Given that the MO basis is orthonormal, P_{pq}^{target} can be used to give the target density's gross Mulliken populations partitioned into the current MO basis. With this in mind, the PMOM and PIMOM models define the modified aufbau metric, s_p, as

$$s_p = \sum_{q} P_{pq}^{target}. \quad (7)$$

The non-aufbau ordering using Equation (7) should be the same as with Equation (3), though the metric expressions and resulting values are not the same. Importantly, the derivation of Equation (7) suggests a unique approach to derive a specific non-aufbau metric among the multiple that have previously appeared in the literature. This work demonstrates that the projection-based approach yields the desired performance in the vast majority of cases, unlike alternative overlap-based metrics (vide infra).

The projection based framework leading to Equation (7) also provides a convenient connection to population analysis. In particular, the values evaluated in Equation (7) are the gross electron populations of the target wave function in the basis of current Fock eigenvectors using both Mulliken and Löwdin partitioning schemes (since the MO basis is orthonormal). As a result, in cases where the current set of occupied MOs results in the same electron density as the target system,

$$n_{el} = \sum_{i} s_i, \quad (8)$$

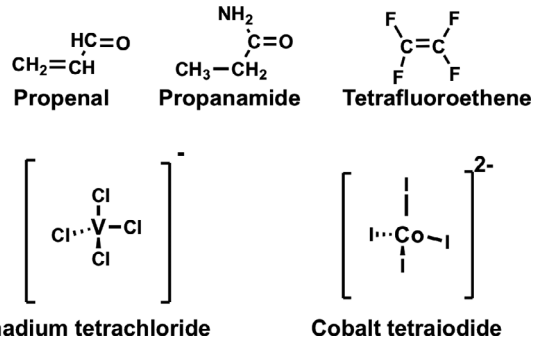

FIGURE 2 Molecules used in calculations on singly excited states

TABLE 2 Values of the N_{virt} metric for singly excited states

Molecule	Model chemistry	PMOM	PIMOM
Propenal	B3LYP/Def2TZVP	0.1 | 0.1	0.1 | 0.1
	HF/Def2TZVP	0.4 | 0.1	0.4 | 0.0
Propanamide	B3LYP/Def2TZVP	0.0 | 0.0	0.0 | 0.0
	HF/Def2TZVP	0.6 | 0.1	0.6 | 0.1
Tetrachloroethane	B3LYP/Def2TZVP	0.0 | 0.0	0.0 | 0.0
	HF/Def2TZVP	0.0 | 0.0	0.0 | 0.0
Nitrobenzene	B3LYP/Def2TZVP	0.0 | 0.0	0.0 | 0.0
	HF/Def2TZVP	1.0 | 0.1	0.0 | 0.0
Vanadium tetrachloride	B3LYP/Def2TZVP	0.2 | 0.0	0.2 | 0.0
	HF/Def2TZVP	0.6 | 0.1	0.6 | 0.1
Cobalt tetraiodide	B3LYP/Def2TZVP	0.0 | 0.3	0.0 | 0.3
	HF/Def2TZVP	0.0 | 0.6	0.0 | 0.6

Note: Values corresponding to the α and β spin–orbital spaces are separated by a vertical pipe.

TABLE 1 Number of SCF iterations required to converge to the targeted singly excited state

Molecule	Model chemistry	Transition	MOM	IMOM	PMOM	PIMOM
Propenal	B3LYP/Def2TZVP	$n \rightarrow \pi^*$	f	f	15	15
	HF/Def2TZVP	$n \rightarrow \pi^*$	f	f	18	18
Propanamide	B3LYP/Def2TZVP	$n \rightarrow \pi^*$	f	f	19	19
	HF/Def2TZVP	$n \rightarrow \pi^*$	f	f	32	31
Tetrafluoroethene	B3LYP/Def2TZVP	$\pi \rightarrow 3s$	f	f	11	11
	HF/Def2TZVP		f	18	16	16
Nitrobenzene	B3LYP/Def2TZVP	$\pi \rightarrow \pi^*$	f	f	29	21
	HF/Def2TZVP	$\pi \rightarrow \pi^*$	f	f	v.c	44
Vanadium tetrachloride	B3LYP/LANL2DZ	$^4T_2$	f	f	19	19
	HF/LANL2DZ	$^4T_2$	f	f	13	13
Cobalt tetraiodide	B3LYP/LANL2DZ	$^4T_2$	f	f	13	13
	HF/LANL2DZ	$^4T_2$	f	f	16	16

Note: The failure of the SCF procedure to converge to either the target or any solution is indicated with the letter "f," whereas variational collapse is indicated by "v.c".

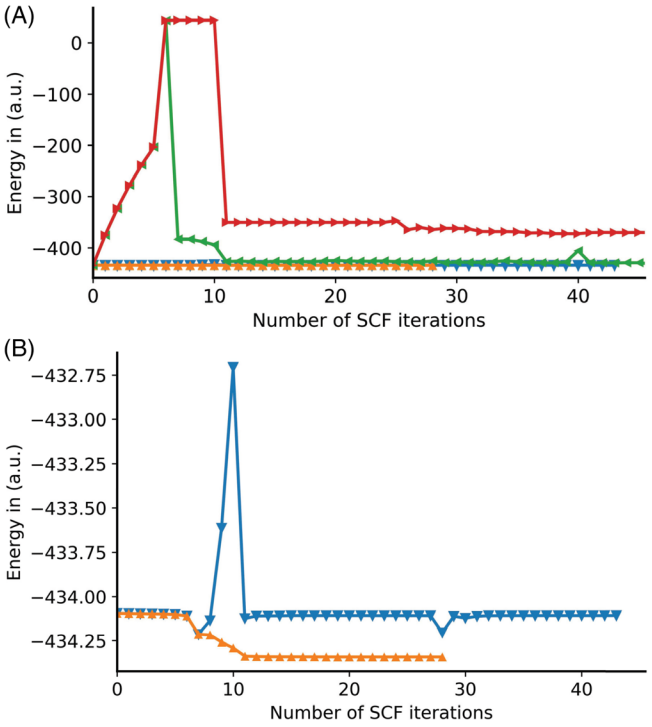

FIGURE 3 Energy convergence to SCF solutions for the excited state of nitrobenzene with MOM (red traces), IMOM (green traces), PMOM (orange traces), and PIMOM (blue traces). Plot (A) shows the results of all the approaches while (B) shows PMOM and PIMOM only. The first 45 cycles are shown. MOM and IMOM did not converge after 500 cycles, PMOM collapsed to the ground state after 27 cycles, and PIMOM converged after 44 cycles

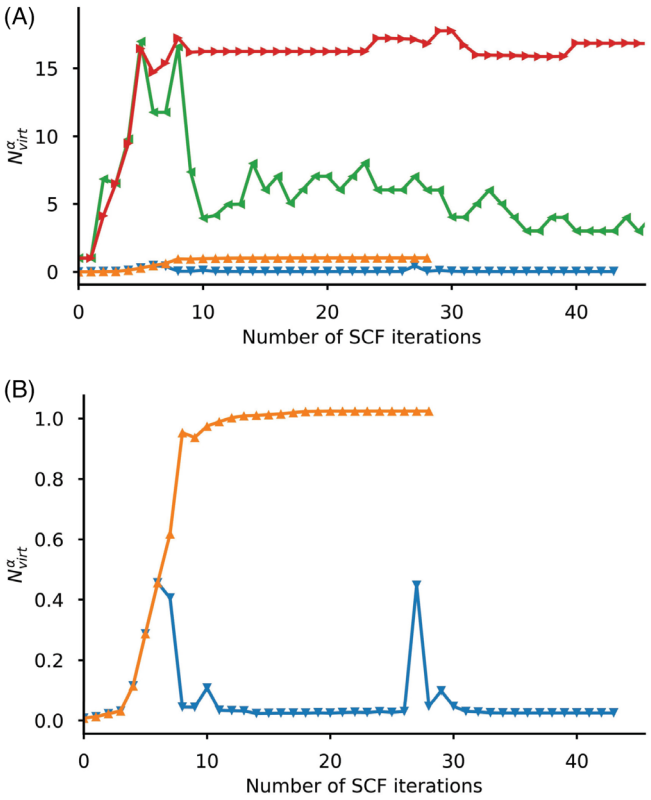

FIGURE 4 N^{α}_{virt} metric at each SCF iteration for the excited state of nitrobenzene with MOM (red traces), IMOM (green traces), PMOM (orange traces), and PIMOM (blue traces). Plot (A) shows the results of all the approaches while (B) shows PMOM and PIMOM only. The first 45 cycles are shown. MOM and IMOM did not converge after 500 cycles, PMOM collapsed to the ground state after 27 cycles, and PIMOM converged after 44 cycles

where n_{el} is the number of electrons. This observation suggests a simple metric for quantifying agreement between the current and target electron densities. Specifically, we define N_{virt} as the projection of the current virtual MOs onto the target system's occupied MOs,

$$N_{virt} = n_{el} - \sum_i s_i = \sum_a s_a, \tag{9}$$

where N_{virt} is in units of electrons. We note the conceptual similarity of our N_{virt} metric with the excitation number described by Gill and coworkers and promotion number by Head-Gordon et al.[40,60,61] In all cases, these different metrics use changes in electron density (in units of electrons) to describe differences between wave functions (or determinants).

3 | NUMERICAL TESTS

The MOM, IMOM, PMOM, and PIMOM methods have been implemented in a local development version of the Gaussian suite of electronic structure programs.[62] To demonstrate and validate PMOM and PIMOM we considered representative sets of singly excited states, double excited states, and ionized states. For the purposes of this study, MOM and IMOM are used to refer to the use of Equation (1) for the non-aufbau metric. We also point out that the performance of PMOM and PIMOM qualitatively mirrors results one would obtain using Equation (3) as the non-aufbau metric.

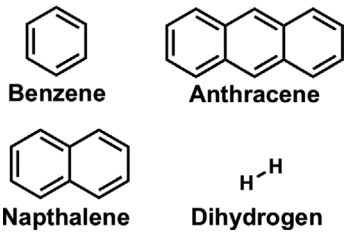

FIGURE 5 Molecules used in calculations on doubly excited state calculations

In all reported results below, the SCF is converged using the direct inversion in the iterative subspace (DIIS) algorithm.[63] We note that actual SCF convergence behavior may be sensitive to the specific DIIS extrapolation scheme employed. The results given below used a combination of commutator-based and energy-based DIIS.[64] In preliminary tests, we also carried out calculations using commutator and

TABLE 3 Number of SCF iterations required to converge to the doubly excited target state

Molecule	Model chemistry	State	MOM	IMOM	PMOM	PIMOM
Benzene	BLYP/6-311G*	$5\,^1A_g$	f	f	9	9
	HF/6-311G*	$5\,^1A_g$	f	f	10	10
Naphthalene	BLYP/6-311G*	$4\,^1A_g$	9	f	9	9
	HF/6-311G*	$4\,^1A_g$	f	f	11	11
Anthracene	BLYP/6-311G*	$2\,^1A_g$	f	f	12	12
	HF/6-311G*	$2\,^1A_g$	f	f	14	14

Note: The failure of the SCF procedure to converge to either the target or any solution is indicated with the letter "f".

energy DIIS separately. Those tests yielded similar convergence behavior for all three schemes.

Converged electronic structures were characterized by visualization of occupied MOs and using a modified form of the natural ionization orbital (NIO) program by Hratchian and coworkers.[65–67] Further assessment was carried out by calculation of Δ-SCF results. Initial guess MOs were selected based on the ground-state, Hartree–Fock (HF)-optimized reference. Excited state guesses were generated by obeying the excited state orbital-symmetry, i.e. a pair of the converged ground state orbitals were permuted to yield the correct symmetry of the desired excited state.

The sub-sections below consider different categories of benchmark systems, as discussed above. The performance for each of the MOM, IMOM, PMOM, and PIMOM approaches was assessed using the number of SCF iterations needed to converge to the desired electronic structure. Calculations were considered failed if convergence was not achieved within 500 iterations. The letter "f" is used below to indicate SCF calculation that converged to an incorrect state or did not converge within 500 iterations. Calculations that incorrectly converged to the ground state solution were characterized as a variational collapse result and are recorded as "v.c." Importantly, we note that "f" and "v.c." results may be dependent on the initial guess wave function and the details of the SCF optimization algorithm. In particular, we note that more sophisticated approaches for preparing the initial guess wave function may yield success for cases that have "f" or "v.c." results in this work.

3.1 | Single excitations

A set of representative molecules for the calculation of single excited states, shown in Figure 2, were selected from the literature.[46,68] All computations were carried out using the Hartree–Fock and B3LYP methods in combination with the Karlsruhe basis set Def2-TZVP (see Table 1). When the various tested SCF driver techniques successfully led to convergence to the desired electronic state, the resulting Δ-SCF excitation energies were in good agreement with reference values (see Table S1).

MOM failed to access any of the desired states in this test set. IMOM also failed to locate the desired electronic structure in most cases, though IMOM did converge to the correct structure for the $\pi \rightarrow 3s$ tetrafluoroethene excited state at the HF level. PMOM was able to access the desired states for all molecules except nitrobenzene at the HF level, where the calculation exhibited variational collapse to the ground state solution. PIMOM, on the other hand, successfully led to SCF solutions corresponding to all desired states with both model chemistries. Though IMOM, PMOM, and PIMOM are all able to converge to the same excited state for many of the included test molecules, the number of SCF iterations needed to converge in each case varied. In cases where different algorithms converge to the desired excited state, the number of SCF iterations requited to converge to the target state was relatively consistent.

TABLE 4 Values of the N_{virt} metric for the computed doubly excited states

Molecule	Model chemistry	PMOM	PIMOM
Benzene	BLYP/6-311G*	0.0	0.0
	HF/6-311G*	0.0	0.0
Naphthalene	BLYP/6-311G*	0.0	0.0
	HF/6-311G*	0.0	0.0
Anthracene	BLYP/6-311G*	0.0	0.0
	HF/6-311G*	0.1	0.1

The N_{virt} value, Equation (9), is an additional metric to evaluate converged states and is reported for all cases studied in Table 2 (see Table S5). In the case of the MOM and IMOM methods, the value of N_{virt} is larger than one. N_{virt} values greater than 1 represent multiple-electron deviations from the user-defined target electronic structure. In the case of the converged states using PMOM and PMOM, the values of N_{virt} are small. Such results support the notion that the projection-based methods perform well at driving the SCF procedure to the desired target electronic structure, even when the initial guess wave function is constructed from straightforward orbital permutations of a related ground state calculation. Fractional N_{virt} values may be interpreted as the result of orbital relaxation as the target electronic structures were defined by an occupied-virtual permutation of the ground state MO structure. As shown in Table 1, PMOM has a v.c. result for nitrobenzene ground state. In this case, $N_{virt} = 1$ indicating that the user-provided target single electron excitation and ground state differ by one occupied-to-virtual transition. For the included

Molecule	Model chemistry	State	MOM	IMOM	PMOM	PIMOM
Propanone	B3LYP/6-311G(d,p)	$2b_1$	f	f	13	13
	HF/6-311G(d,p)	$2b_1$	f	f	16	16
Methanol	B3LYP/6-311G(d,p)	$7a'$	f	f	12	12
	Hf/6-311G(d,p)	$7a'$	f	f	18	18
Pyridine	B3LYP/6-311G(d,p)	$9b_2$	f	f	14	14
	Hf/6-311G(d,p)	$9b_2$	f	f	21	21
Formaldehyde	B3LYP/6-311G(d,p)	$1b_1$	10	10	10	10
	HF/6-311G(d,p)	$1b_1$	13	13	13	13

TABLE 5 Number of SCF iterations required to converge to the correct ionized state

Note: The failure of the SCF procedure to converge to either the target or any solution is indicated with the letter "f".

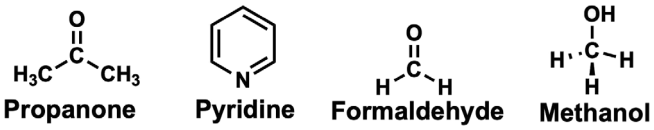

FIGURE 6 Molecules used in calculations on ionized states

vanadium and cobalt complexes, the $^4T_2$ states have previously been included as tests for the guided method by Li and co-workers.[46] The current work demonstrates that PMOM and PIMOM were also able to reproduce the same results.

Figures 3 and 4 show the progress of the SCF procedure for the case of the $\pi \rightarrow \pi^*$ excitation of nitrobenzene. Energy as a function of the SCF cycle number is shown in Figure 3; the metric N_{virt} as a function of the SCF cycle number is presented in Figure 4. As shown in Figure 3A, MOM and IMOM lead to large deviations from the current energy early in the SCF procedure. The SCF energy in these cases eventually diverges from the desired final state energy. This is also reflected in the value of N_{virt}. In both MOM and IMOM calculations, N_{virt} presents iterations with quite large values. These two observations suggest that MOM and IMOM, in the current implementation and using the simple initial guess wave functions employed here, can drift far from the desired solution.

Figures 3 and 4 also show results for PMOM and PIMOM calculations. The behavior of PMOM leads to variational collapse to the ground state with a N_{virt} value of 1.0. This value corresponds to the one electron difference between the desired excited state and converged ground state SCF solutions. Again, the N_{virt} metric provides a useful tool for assessing the behavior of such Δ-SCF methods. On the other hand, PIMOM shows steady convergence to the correct excited state solution. As expected, N_{virt} for the final PIMOM converged wave function is nearly zero.

3.2 | Double excitations

Figure 5 shows a set of arene examples included to study the use of the tested schemes on double-excitation states. This set has been used in earlier work reporting IMOM.[40] We also include the $1\sigma_g^2 \rightarrow 1\sigma_u^2$ excitation in H2 using the augmented mcc-pV8Z basis set with an additional $2f2g$ set of diffuse functions. In all cases, previously reported energy values were reproduced (see, Tables S2 and S3). Table 3 reports our results for the arene molecules. MOM was only able to access one of the targeted states, whereas IMOM was unable to converge to any of the targets. PMOM and PIMOM required the same number of iterations to converge to the same energy values for all states. The values of N_{virt} for this set of molecules, shown in Table 4, are again consistent with our interpretation of N_{virt} (see Table S6). For the converged states, the value of N_{virt} is smaller than 1 and corresponds to orbital relaxation in the excited state.

TABLE 6 Values of the N_{virt} metric for the different ionized excited states computed

Molecule	Model chemistry	PMOM	PIMOM
Propanone	B3LYP/6-311G(d,p)	0.0 | 0.1	0.0 | 0.1
	HF/6-311G(d,p)	0.6 | 0.1	0.6 | 0.1
Methanol	B3LYP/6-311G(d,p)	0.0 | 0.1	0.0 | 0.1
	HF/6-311G(d,p)	0.0 | 0.6	0.0 | 0.6
Pyridine	B3LYP/6-311G(d,p)	0.0 | 0.0	0.0 | 0.0
	HF/6-311G(d,p)	0.1 | 0.2	0.1 | 0.2
Formaldehyde	B3LYP/6-311G(d,p)	0.0 | 0.0	0.0 | 0.0
	HF/6-311G(d,p)	0.0 | 0.1	0.0 | 0.1

Note: Values corresponding to the α and β spin–orbital spaces are separated by a vertical pipe.

3.3 | Ionizations

Ionized states were evaluated by computing the ionization energy corresponding to electron detachment from orbitals other than that of the HOMO of the initial state. Results for a representative set of molecules are presented in Table 5 and Figure 6, showing only PMOM and PIMOM successfully accessed all ionized states and did so within the same number of SCF iterations. MOM and IMOM only converged

to the desired ionized state for formaldehyde. In that particular case, the number of SCF iterations was the same as for PMOM and PIMOM. As in previous cases, the N_{virt} values for the converged states have values less than 1 (Table 6 and Table S7). The ionization energies computed for the converged states are in good agreement with literature values (see Table S4).[69]

4 | CONCLUSIONS

This work described and assessed PMOM and PIMOM projection-based maximum overlap methods. For the systems examined here, PIMOM is a particularly robust member of the maximum overlap method family. In particular, this work has demonstrated that PIMOM can converge to intended electronic structure solutions using relatively simple user-provided initial guess determinants as a target wave function. Specifically, this report used permutations of ground state occupied/virtual MO pairs as initial and target wave functions.

As shown above, PMOM and PIMOM both perform quite well. Indeed, for the cases included here, PMOM and PIMOM are the most consistent of the maximum overlap methods considered. In most cases, PMOM and PIMOM require the same number of iterations to converge. At first glance, this may suggest no apparent advantage from using PIMOM versus PMOM. However, in cases such as nitrobenzene, PMOM exhibits variational collapse and results in optimization to the ground state, which is consistent with previous literature showing that the *initial* guess wave function is generally a better target choice for maximum overlap methods than the evolving wave function from the previous SCF cycle.[40]

The presented N_{virt} metric provides a simple and conceptually convenient measure of agreement between the desired target and the current or final SCF results during a calculation employing a maximum overlap method. In successful calculations, N_{virt} values were close to zero. For the cases in which a maximum overlap method failed to converge to the desired solution, the N_{virt} values comparing a target SCF solution and the final result were greater than 1. And in cases where the final SCF solution resulted from variational collapse, N_{virt} is roughly equal to the number of intended excited electrons. We envision using N_{virt} during a maximum-overlap-method based calculation to identify problematic SCF optimizations early in the iterative process. One could envision incorporating such a metric with tools meant to stabilize the optimization process, such as the recently reported STEP technique.[44]

Although PIMOM has been shown to be a reliable method for converging challenging SCF solutions, questions remain regarding the resemblance between converged PIMOM SCF solutions and molecular electronic states and about limitations when describing wave functions that may be properly multi-determinantal in nature. The presented PIMOM formulation employs a simple form for the projection operator. In some cases, the $\mathcal{P}^{\text{target}}$ operator may not be compactly presentable for a system's Hilbert space. In these systems, one may find degenerate sub-spaces corresponding to a single eigenvalue of the operator containing multiple (perhaps infinite) $|i\rangle\langle i|$-like terms.[70–74] For such cases, two-argument projection operators may be more prudent for the formulation of the PIMOM algorithm. Work exploring such questions is underway.

ACKNOWLEDGMENTS

The development and initial assessment of the presented methods were supported by the National Science Foundation (HPH; Award CHE-1848580), and exploration of the presented methods for the study of excited electronic states was supported by the Department of Energy, Office of Basic Energy Sciences CTC and CPIMS programs (HPH and APJ; Award DE-SC0014437). Computing time was provided in part by the MERCED cluster at UC Merced, which was also supported by the National Science Foundation (Award ACI-1429783).

DATA AVAILABILITY STATEMENT

The data that supports the findings of this study are available in the supplementary material of this article.

ORCID

Aurora Pribram-Jones https://orcid.org/0000-0003-0244-1814
Hrant P. Hratchian https://orcid.org/0000-0003-1436-5257

REFERENCES

[1] A. Dreuw, M. Wormit, *Rev.: Comput. Mol. Sci.* **2015**, *5*, 82.
[2] M. Filatov, *Rev.: Comput. Mol. Sci.* **2015**, *5*, 146.
[3] K. Sneskov, O. Christiansen, *Rev.: Comput. Mol. Sci.* **2012**, *2*, 566.
[4] C. M. Marian, A. Heil, M. Kleinschmidt, *Wiley Interdiscip. Rev.: Comput. Mol. Sci.* **2019**, *9*, e1394.
[5] M. A. Robb, *Theoretical chemistry for electronic excited states*. Vol. 12, Royal Society of Chemistry **2018**, P001.
[6] L. Otis, I. Craig, E. Neuscamman, *J. Chem. Phys.* **2020**, *153*, 234105.
[7] T. S. Hardikar, E. Neuscamman, *J. Chem. Phys.* **2020**, *153*, 164108.
[8] A. Dreuw, M. Head-Gordon, *Chem. Rev.* **2005**, *105*, 4009.
[9] B. J. Coe, J. L. Harries, M. Helliwell, L. A. Jones, I. Asselberghs, K. Clays, B. S. Brunschwig, J. A. Harris, J. Garín, J. Orduna, *J. Am. Chem. Soc.* **2006**, *128*, 12192.
[10] S. R. Stoyanov, J. M. Villegas, A. J. Cruz, L. L. Lockyear, J. H. Reibenspies, D. P. Rillema, *J. Chem. Theory Comput.* **2005**, *1*, 95.
[11] G. Fronzoni, M. Stener, A. Reduce, P. Decleva, *J. Phys. Chem. A* **2004**, *108*, 8467.
[12] C. Lapouge, J. Cornard, *J. Phys. Chem. A* **2005**, *109*, 6752.
[13] L. M. Ramaniah, M. Boero, *Phys. Rev. A* **2006**, *74*, 042505.
[14] A. Marinopoulos, L. Wirtz, A. Marini, V. Olevano, A. Rubio, L. Reining, *Appl. Phys. A: Mater. Sci. Process.* **2004**, *78*, 1157.
[15] A. D. Quartarolo, N. Russo, E. Sicilia, *Chem. Eur. J.* **2006**, *12*, 6797.
[16] D. Varsano, R. Di Felice, M. A. Marques, A. Rubio, *J. Phys. Chem. B* **2006**, *110*, 7129.
[17] M. A. Marques, X. López, D. Varsano, A. Castro, A. Rubio, *Phys. Rev. Lett.* **2003**, *90*, 258101.
[18] B. J. Coe, J. A. Harris, B. S. Brunschwig, I. Asselberghs, K. Clays, J. Garín, J. Orduna, *J. Am. Chem. Soc.* **2005**, *127*, 13399.
[19] R. J. Cave, K. Burke, E. W. Castner, *J. Phys. Chem. A* **2002**, *106*, 9294.
[20] D. Jacquemin, E. A. Perpète, G. Scalmani, M. J. Frisch, X. Assfeld, I. Ciofini, C. Adamo, *J. Chem. Phys.* **2006**, *125*, 164324.
[21] C. J. Jamorski, M. E. Casida, *J. Phys. Chem. B* **2004**, *108*, 7132.
[22] D. Rappoport, F. Furche, *J. Am. Chem. Soc.* **2004**, *126*, 1277.
[23] D. J. Tozer, *J. Chem. Phys.* **2003**, *119*, 12697.
[24] C. Jamorski Jödicke, H. P. Lüthi, *J. Am. Chem. Soc.* **2003**, *125*, 252.
[25] Z.-L. Cai, K. Sendt, J. R. Reimers, *J. Chem. Phys.* **2002**, *117*, 5543.

[26] S. Grimme, M. Parac, *Chem. Phys. Chem.* **2003**, *4*, 292.
[27] D. J. Tozer, R. D. Amos, N. C. Handy, B. O. Roos, L. Serrano-Andres, *Mol. Phys.* **1999**, *97*, 859.
[28] A. L. Sobolewski, W. Domcke, *Chem. Phys.* **2003**, *294*, 73.
[29] A. Dreuw, G. R. Fleming, M. Head-Gordon, *J. Phys. Chem. B* **2003**, *107*, 6500.
[30] P. S. Bagus, Tech. Rep., Chicago Univ Il Lab of Molecular Structure and Spectra **1964**.
[31] J. Broughton, P. Bagus, *J. Electron Spectrosc. Relat. Phenom.* **1980**, *20*, 127.
[32] L. Dardenne, N. Makiuchi, L. Malbouisson, J. Vianna, *Int. J. Quantum Chem.* **2000**, *76*, 600.
[33] E. R. Davidson, L. Z. Stenkamp, *Int. J. Quantum Chem.* **1976**, *10*, 21.
[34] R. McWeeny, *Mol. Phys.* **1974**, *28*, 1273.
[35] R. J. Bartlett, Y. Öhrn, *Theor. Chim. Acta* **1971**, *21*, 215.
[36] H.-Z. Ye, M. Welborn, N. D. Ricke, T. Van Voorhis, *J. Chem. Phys.* **2017**, *147*, 214104.
[37] M. McCourt, J. W. McIver Jr., *J. Comput. Chem.* **1987**, *8*, 454.
[38] J. Liu, Y. Zhang, P. Bao, Y. Yi, *J. Chem. Theory Comput.* **2017**, *13*, 843.
[39] P. Corrêa De Mello, M. Hehenberger, M. Zernert, *Int. J. Quantum Chem.* **1982**, *21*, 251.
[40] G. M. Barca, A. T. Gilbert, P. M. Gill, *J. Chem. Theory Comput.* **2018**, *14*, 1501.
[41] G. M. Barca, A. T. Gilbert, P. M. Gill, *J. Chem. Phys.* **2014**, *141*, 111104.
[42] A. T. Gilbert, N. A. Besley, P. M. Gill, *J. Phys. Chem. A* **2008**, *112*, 13164.
[43] D. Hait, M. Head-Gordon, *J. Chem. Theory Comput.* **2020**, *16*, 1699.
[44] K. Carter-Fenk, J. M. Herbert, *J. Chem. Theory Comput.* **2020**, *16*, 5067.
[45] Y. Mei, W. Yang, *J. Chem. Phys.* **2019**, *150*, 144109.
[46] B. Peng, B. E. Van Kuiken, F. Ding, X. Li, *J. Chem. Theory Comput.* **2013**, *9*, 3933.
[47] R. Flores-Moreno, V. Zakrzewski, J. Ortiz, *J. Chem. Phys.* **2007**, *127*, 134106.
[48] O. Sinanoglu, D. Fu-tai Tuan, *Annu. Rev. Phys. Chem.* **1964**, *15*, 251.
[49] P. G. Lykos, H. N. Schmeising, *J. Chem. Phys.* **1961**, *35*, 288.
[50] E. R. Sayfutyarova, Q. Sun, G. K.-L. Chan, G. Knizia, *J. Chem. Theory Comput.* **2017**, *13*, 4063.
[51] C.-G. Zhan, *Int. J. Quantum Chem.* **1987**, *32*, 1.
[52] Z. Maksic, M. Eckert-Maksic, M. Randic, *Theor. Chim. Acta* **1971**, *22*, 70.
[53] D. H. Kobe, *Phys. Rev. C* **1971**, *3*, 417.
[54] F. Weinhold, T. Brunck, *J. Am. Chem. Soc.* **1976**, *98*, 3745.
[55] H. Meldner, J. Perez, *Phys. Rev. C* **1973**, *7*, 2158.
[56] J. Cioslowski, M. Challacombe, *Int. J. Quantum Chem.* **1991**, *40*, 81.
[57] N. A. Besley, A. T. Gilbert, P. M. Gill, *J. Chem. Phys.* **2009**, *130*, 124308.
[58] A. Baiardi, L. Paoloni, V. Barone, V. Zakrzewski, J. Ortiz, *J. Chem. Theory Comput.* **2017**, *13*, 3120.
[59] W. J. Hehre, L. Radom, P. von Schleyer, J. Pople, *AB INITIO Molecular Orbital Theory*, 1st ed., Wiley, New York **1986**.
[60] G. M. Barca, A. T. Gilbert, P. M. Gill, *J. Chem. Theory Comput.* **2018**, *14*, 9.
[61] M. Head-Gordon, A. M. Grana, D. Maurice, C. A. White, *J. Phys. Chem.* **1995**, *99*, 14261.
[62] M. J. Frisch, G. W. Trucks, H. B. Schlegel, G. E. Scuseria, M. A. Robb, J. R. Cheeseman, G. Scalmani, V. Barone, G. A. Petersson, H. Nakatsuji, et al., *Gaussian Development Version REVISION I.09*, Gaussian Inc., Wallingford, CT **2016**.
[63] P. Pulay, *J. Comput. Chem.* **1982**, *3*, 556.
[64] K. N. Kudin, G. E. Scuseria, E. Canés, *J. Chem. Phys.* **2002**, *116*, 8255.
[65] L. M. Thompson, H. Harb, H. P. Hratchian, *J. Chem. Phys.* **2016**, *144*, 204117.
[66] H. Harb, H. P. Hratchian, *J. Chem. Phys.* **2021**, *154*, 084104.
[67] H. Harb, H. P. Hratchian, *Natural Ionization Orbitals*, HratchianGroup/niorep, **2020**. https://github.com/
[68] P. Ramos, M. Pavanello, *J. Chem. Phys.* **2018**, *148*, 144103.
[69] H. Corzo, A. Galano, O. Dolgounitcheva, V. Zakrzewski, J. Ortiz, *J. Phys. Chem. A* **2015**, *119*, 8813.
[70] H. Kim, A. Nassimi, R. Kapral, *J. Chem. Phys.* **2008**, *129*, 084102.
[71] A. Kelly, R. van Zon, J. Schofield, R. Kapral, *J. Chem. Phys.* **2012**, *136*, 084101.
[72] G. E. Scuseria, C. A. Jiménez-Hoyos, T. M. Henderson, K. Samanta, J. K. Ellis, *J. Chem. Phys.* **2011**, *135*, 124108.
[73] I. G. Ryabinkin, S. N. Genin, A. F. Izmaylov, *J. Chem. Theory Comput.* **2018**, *15*, 249.
[74] A. F. Izmaylov, *J. Phys. Chem. A* **2019**, *123*, 3429.

SUPPORTING INFORMATION

Additional supporting information may be found in the online version of the article at the publisher's website.

How to cite this article: H. H. Corzo, A. Abou Taka, A. Pribram-Jones, H. P. Hratchian, *J. Comput. Chem.* **2022**, *43*(6), 382. https://doi.org/10.1002/jcc.26797